

Article

# Open-Sea Testing of Two-Phase Marine Ramjet Propulsion

Shlomit Valensi and Alon Gany \* 

Faculty of Aerospace Engineering, Technion—Israel Institute of Technology, Haifa 32000, Israel; svalensi@gmail.com

\* Correspondence: gany@tx.technion.ac.il

**Abstract:** Open-sea testing of a two-phase marine ramjet vehicle has been conducted. This experimental phase was accomplished following comprehensive theoretical research. The concept of two-phase marine ramjet propulsion consists of a submerged propulsor acquiring water through an inlet due to the vehicle's motion. Thrust is generated by injecting and dispersing air (or gas) bubbles within the water flowing through the propulsion unit channel and expelling a jet of the two-phase flow through an exit nozzle. The bubbles injected into the internal flow transmit their expansion work to the outgoing jet, resulting in an increase in the jet velocity, hence generating thrust. The article briefly describes the thrust generation concept, then it presents the overall system and thrust units attached to the test vessel, and finally, it summarizes the open-sea experimental results. Good correspondence between the theoretical prediction and actual test data is shown, revealing the feasibility of the two-phase ramjet concept at the low to intermediate cruise velocity range and a smaller relative thrust margin over the hydrodynamic resistance at the high-speed range.

**Keywords:** two-phase flow; marine ramjet; bubbly jet; two-phase jet propulsion



**Citation:** Valensi, S.; Gany, A. Open-Sea Testing of Two-Phase Marine Ramjet Propulsion. *J. Mar. Sci. Eng.* **2023**, *11*, 2220. <https://doi.org/10.3390/jmse11122220>

Academic Editor: Sergey M. Frolov

Received: 16 October 2023

Revised: 9 November 2023

Accepted: 20 November 2023

Published: 23 November 2023



**Copyright:** © 2023 by the authors. Licensee MDPI, Basel, Switzerland. This article is an open access article distributed under the terms and conditions of the Creative Commons Attribution (CC BY) license (<https://creativecommons.org/licenses/by/4.0/>).

## 1. Introduction

The ramjet is a jet engine acquiring fluid matter from the surrounding ambient medium due to the vehicle motion without the use of moving mechanical devices such as pumps or compressors. The incoming flow is used as a major part of the working fluid; after adding energy within the propulsor (typically by fuel combustion in the case of an aeronautical engine), thrust is generated as a result of the expulsion of a high-speed jet through an exhaust nozzle. The pressure inside the propulsor is determined by the conversion of the dynamic (ram) pressure component of the incoming fluid into static pressure inside the propulsor, allowing expansion and acceleration of the working fluid when exhausted to the surroundings. Typically, ramjet propulsion is associated with aeronautical flight vehicles moving in the air, where the incoming air serves as both the main component of the working fluid and the oxidizer for the combustion process with the supplied fuel.

The marine two-phase water-air ramjet consists of ingesting water through an inlet due to the vessel motion, adding energy to the working fluid via the introduction of compressed air bubbles, and accelerating the two-phase mixture through an exhaust nozzle, thus generating thrust. The main advantages of such a thruster are the absence of moving parts (such as pumps), power transmission (from the bubbles to the water) pneumatically instead of mechanically, and no internal cavitation problems because the internal pressure is typically higher than the atmospheric pressure.

The dynamic behavior of two-phase water-air bubbly flows has been investigated for quite a long time. One of the first compressible two-phase flow research (Tangren et al. [1]) analyzed such flow through a nozzle assuming thermodynamic equilibrium between the phases. They conducted certain experiments measuring pressure and thrust. Muir and Echhorn [2] performed a similar analysis by studying the dynamics of a bubbly flow in a vertical tube. Using a two-dimensional transparent flow facility consisting of

a straight mixing chamber and nozzle, they could detect the pressure and velocity variations. Analysis of two-phase bubbly flows was discussed in detail by Soo [3], Wallis [4], Van Wijngaarden [5], and Brennen [6]. A comprehensive analysis of bubbly flows with heat, mass, and momentum interactions including wall friction as well as evaporation and condensation effects, was performed by Albagli and Gany [7]. They presented the variation of water and bubble velocities, bubble temperature in case of introduction at high temperature, bubble size, gas-phase volume fraction, and Mach number along a nozzle, revealing the possibility of choking and showing that wall friction results in lower exit velocity. Mor and Gany [8] analyzed two-phase homogeneous bubbly nozzle flow considering friction and mass addition. They received closed-form solutions for certain cases, presenting the variation of different flow parameters as a function of Mach number. Several researchers related their investigation specifically to two-phase marine ramjet performance (Mottard and Shoemaker [9], Witte [10]). The analysis of the latter was extended to conditions where the two phases may have different velocities. Albagli and Gany [11] presented an analysis of a high-speed bubbly water ramjet, presenting a specific propulsor configuration, showing the development of flow parameters along the axis, and evaluating the specific impulse compared to that of a perfect gas jet. Varshay and Gany [12,13] registered patents describing the geometry and operating principles of the two-phase ramjet. Basic analysis predicting the performance of a two-phase ramjet, including the effect of different parameters such as cruise velocity, air-bubble mass fraction, and the efficiency of sub-processes, was presented by Gany [14]. Elaboration will be given below. Early design and analysis were performed with the aim of providing two-phase jet propulsion to a hydrofoil craft called MARJET (Pierson [15]). Certain measurements took place demonstrating the possibility of substantial thrust. However, the publication does not provide evidence that the actual MARJET vehicle has been operated in practice. Mor and Gany [16] presented a performance map of a two-phase marine ramjet, revealing the predicted thrust and efficiency versus cruise speed for a range of airflow rates and mass fractions. That research can serve as a convenient tool for determining the operating parameters of practical vehicles. More work on air-augmented waterjet has been conducted in the last two decades, e.g., Dynaflo's research [17–19], Gowing et al. [20], Fu et al. [21], Liu et al. [22], and Zhang et al. [23]. They included certain analytical aspects, numerical calculations, and experiments, typically in static systems with transparent walls allowing visualization of the flow development and phenomena. Some of those works have been related to pump-operated waterjets. The ram rocket, a rocket-based water-breathing ramjet concept, has been investigated by Eisen and Gany [24–26]. Unlike the bubbly jet, where the gas mass fraction in the two-phase flow is a fraction of the percent of the water amount, the ram rocket concept aims at augmenting the thrust and energetic performance compared to that of a rocket at very high underwater cruise velocities. The incoming water is converted to steam when mixing with the high-temperature combustion products and its amount (mass-wise) is comparable to that of the combustion products. The mixture is exhausted through a nozzle generating substantially higher thrust than that of a rocket motor, mainly due to the higher jet mass flow rate. A different concept of marine ramjet, the pulse detonation hydroramjet, was recently studied by Frolov et al. [27]. They presented an experimental investigation revealing positive average thrust and good performance. However, the resulting thrust was pulsating according to the frequency of the pulses in the detonation tube. It is noted that none of the surveyed publications have included performance characterization in an actual cruising vessel.

The objective of this research is to test the actual propulsion performance of the two-phase marine ramjet in open-sea cruise conditions of a full-scale vessel and to compare it to theoretical prediction.

## 2. Brief Theoretical Analysis

Analytical considerations of the operating principle and performance of the two-phase water-air marine ramjet will be summarized below following Gany [14]. A schematic illustration is presented in Figure 1.

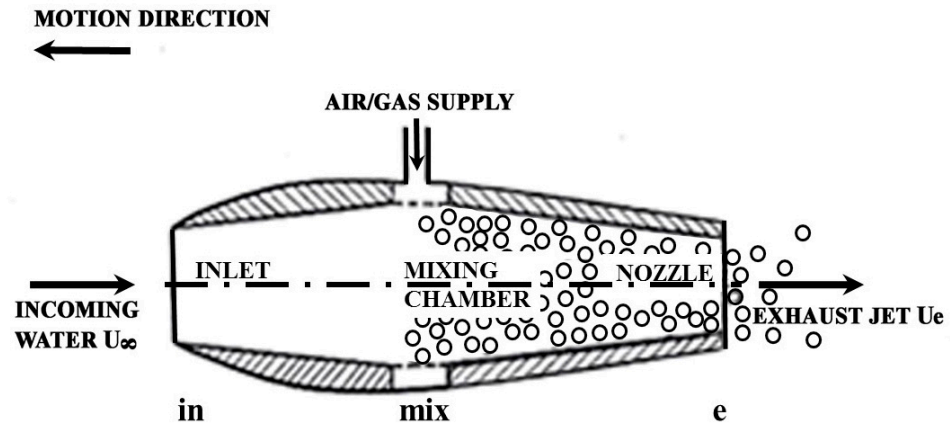


Figure 1. Schematic illustration of the marine two-phase bubbly ramjet.

During cruising, water enters into the marine ramjet propulsor due to the vehicle’s motion (similar to the ingestion of air in the aeronautical ramjet). The incoming water slows down within the inlet diffuser, whose cross-section increases gradually in the axial direction. The decrease in water flow velocity results in an increase in the (static) pressure. The introduction of compressed air (at a pressure approximately equal to the internal pressure in the mixing chamber) is conducted along a section starting from a certain cross-section. The air comes from a source external to the propulsor. It is introduced in the form of small bubbles, ideally distributed uniformly within the water flow in the internal channel. After the mixing section, the channel cross-section decreases in the axial direction, forming an exit nozzle (either converging or converging-diverging). Assuming one-dimensional flow expanding to the ambient pressure, and accounting for the fact that the mass flow rate of the air  $\dot{m}_a$  is almost negligible (less than 1%) compared to that of the water,  $\dot{m}_a \ll \dot{m}_w$ , one obtains a simplified thrust equation:

$$F = \dot{m}(U_e - U_\infty) \tag{1}$$

where  $F$  is the thrust,  $U_e$  and  $U_\infty$  are the exit jet and cruise velocities, respectively, and the overall mass flow rate  $\dot{m}$  is approximately equal to the water flow rate  $\dot{m}_w$ . The ideal thermodynamic power cycle is presented in Figure 2 on a temperature-entropy (T-S) thermodynamic diagram in relation to the air.

Air at ambient temperature  $T_a$  and pressure  $P_a$  (station **a**) is compressed by an external compressor to a pressure  $P_{comp}$  (station **comp**), which is equal to the mixing chamber pressure,  $P_{comp} = P_{mix}$ . Introduced into the water stream within the mixing chamber, the air bubbles lose their thermal energy (approximately at constant pressure), eventually reaching the water temperature (which is assumed to be equal to the ambient temperature), as indicated by the line between station **comp** and station **mix** in Figure 2. Moving along the nozzle, the air bubbles expand isothermally from the mixing chamber pressure  $P_{mix}$  to the exit pressure, which is equal to the ambient pressure  $P_a$ . During that process, the air absorbs energy from the surrounding water.

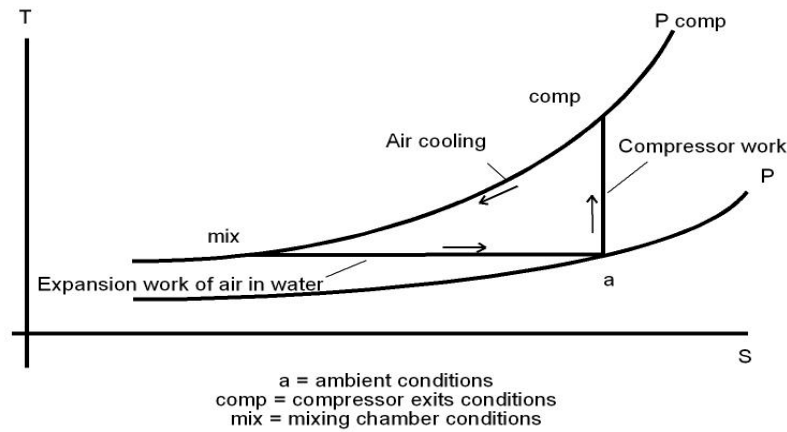


**Figure 2.** Thermodynamic temperature-entropy (T-S) diagram of the ideal power cycle of the two-phase marine ramjet per unit mass of air (after Gany [14]).

The invested work in ideal (isentropic) compression per unit mass of air is:

$$w_{\text{comp}} = C_p T_a \left( r^{\frac{\gamma-1}{\gamma}} - 1 \right) \tag{2}$$

where  $r$  is the compression ratio:

$$r = P_{\text{comp}} / P_a \tag{3}$$

Expressing the specific heat of air  $C_p$  in terms of the specific gas constant  $R$ :

$$C_p = \frac{\gamma R}{\gamma - 1} \tag{4}$$

and accounting for the temperature increase during compression

$$T_{\text{comp}} = T_a r^{\frac{\gamma-1}{\gamma}} \tag{5}$$

one obtains an expression for the ideal invested compression work per unit mass of air:

$$w_{\text{comp}} = \frac{\gamma R T_a}{\gamma - 1} \left( r^{\frac{\gamma-1}{\gamma}} - 1 \right) \tag{6}$$

In the case of air,  $\gamma = 1.4$  and  $R = 287 \text{ J}/(\text{kg K})$ .

Mixing with the water, the hot compressed air rapidly loses its thermal energy, attaining the water temperature which is equal to the ambient temperature. However, while moving along the channel toward the exit from  $P_{\text{comp}}$  to  $P_a$ , the air bubbles absorb energy from the surrounding water and remain in constant temperature, transmitting their isothermal expansion work (per unit mass of air) to the flow:

$$w_{\text{exp}} = R T_a \ln r \tag{7}$$

We define the thermodynamic power cycle efficiency as the ratio between the isothermal work delivered to the flow and the invested isentropic work in the external compressor:

$$\eta_{\text{cycle}} = \frac{w_{\text{exp}}}{w_{\text{comp}}} = \frac{\ln r}{\frac{\gamma}{\gamma-1} \left( r^{\frac{\gamma-1}{\gamma}} - 1 \right)} \tag{8}$$

Since the isothermal expansion work is always smaller than the isentropic compression work, the power cycle efficiency is always smaller than unity, and it decreases with increasing the cruise velocity, as can be seen in Figure 3.

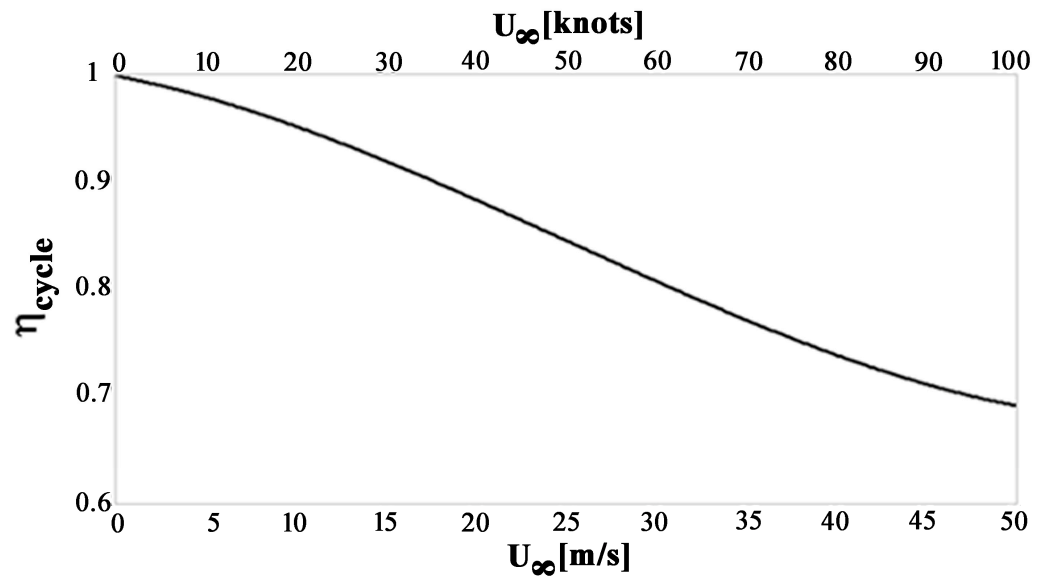


Figure 3. Cycle efficiency vs. cruise speed for the ideal power cycle (after Gany [14]).

Energy balance in the two-phase marine ramjet, using  $\dot{m}_a \ll \dot{m}_w$  and accounting for total pressure or kinetic energy recovery in the diffuser  $K_r$  and for isothermal expansion efficiency of the air bubbles  $\eta_b$ , can be expressed for a unit mass of water, assuming one-dimensional flow and local equal pressure and velocity of the water and air-bubble phases:

$$\frac{U_e^2}{2} = K_r \frac{U_\infty^2}{2} + \eta_{\text{cycle}} \eta_b \mu W_{\text{comp}} \tag{9}$$

where  $\mu$  is the air-to-water mass flow rate ratio,  $\dot{m}_a / \dot{m}_w$ .

Assuming complete total kinetic energy recovery in the diffuser,  $K_r = 1$ , and ideal bubble expansion efficiency,  $\eta_b = 1$ , one can rewrite Equation (9) as follows:

$$\frac{U_e^2}{2} = \frac{U_\infty^2}{2} + \mu RT_a \ln r \tag{10}$$

The kinetic energy of the exhaust jet will be larger than that of the incoming water by the added expansion energy, which is equal to  $\mu RT_a \ln r$  per unit mass of water, at the most (when  $\eta_b = 1$ ).

The static pressure in the mixing chamber is a function of the incoming water stagnation (total) pressure  $P_t$ . Its maximum value, when all the dynamic (ram) pressure of the incoming water is converted into static pressure, is:

$$P_{\text{comp,max}} = P_a + \frac{1}{2} \rho_w U_\infty^2 = P_t \tag{11}$$

For a cruise speed of 10 m/s (20 knots) it may attain 1.5 bars (absolute), namely, under such conditions the pressure ratio is approximately  $r = 1.5$ , according to Equation (11) with the water density  $\rho_w = 1000 \text{ kg/m}^3$ . In practice, the static pressure in the mixing chamber is smaller than the total pressure, even with no pressure losses, because the flow in the mixing section has a certain velocity according to the area ratio between the mixing chamber and the inlet cross sections.

There is another factor limiting the energy added to the exit jet. It is the air volume fraction  $\alpha$ , which enables the existence of a bubbly flow. The maximum volume fraction is at the exit plain, where the pressure is the atmospheric pressure. It can be expressed in terms of the air-to-water mass ratio (see [8]):

$$\alpha_e = \frac{\mu}{\mu + \rho_{a,e} / \rho_w} \tag{12}$$

The air volume fraction for a bubbly flow regime should typically be of the order of 50–70%, hence,  $\mu = 0.1\text{--}0.3\%$  approximately.  $\alpha = 74\%$  is the maximum theoretical volumetric packing of monodisperse (unisize) spherical bubbles, corresponding to  $\mu = 0.34\%$ , indicating roughly the high limit for such bubbly flow. Nevertheless, multiple-size bubbles (which is often the case) may exhibit much higher volumetric (and hence, mass fraction) packing. Thus, the addition beyond this volume fraction can still contribute to the thrust. See the correlation between  $\mu$  and  $\alpha_e$  in Table 1.

**Table 1.** The correlation between the mass and volume fractions of air in two-phase air-water flow.

Vol Fraction at Exit Plain, $\alpha_e$	$\mu$
40%	0.08%
50%	0.12%
60%	0.18%
70%	0.28%
74%	0.34%
80%	0.48%
85%	0.68%
90%	1.08%
95%	2.28%

The example presented before, i.e.,  $\alpha_e$  between 50% and 70% and cruise speed of 10 m/s, would yield relative additional kinetic energy to the exit jet of 70% to 200% approximately, compared to that of the incoming flow. However, the relative additional energy decreases with increasing the cruise speed. At 50 m/s it would be only about 20% to 60%, indicating a substantial reduction in the relative increase in kinetic energy of the exhaust jet. Furthermore, since the static pressure in the mixing chamber is lower than the total pressure (according to the area ratio between the two cross-sections and the one-dimensional continuity equation for the incompressible flow of water), the pressure ratio for the expanding air bubbles will be lower, decreasing the contribution to the exit jet kinetic energy, Equation (13):

$$P_{mix} = P_t - \frac{1}{2} \rho_w U_\infty^2 (A_{in} / A_{mix})^2 \tag{13}$$

For instance, in the case of  $A_{mix} / A_{in} = 2$ ,  $P_{mix} = P_t - \frac{1}{8} \rho_w U_\infty^2 = 1.38$  bar, and  $r = 1.38$  approximately; then the bubble expansion contribution would ideally be about 55% to 165% (still high) for a cruise speed of 10 m/s, and only 16% to 50% for a cruise speed of 50 m/s. In addition, although the ramjet thrust increases with the cruise velocity, both because of the increase in the water flow rate (linearly with the cruise velocity for a given inlet cross-section) and because of the higher pressure-ratio, the hydrodynamic resistance (drag) has a higher dependence on the cruise speed (relative to  $U_\infty^2$ ):

$$D = \frac{1}{2} \rho_w U_\infty^2 S_{wet} C_D \tag{14}$$

where  $S_{wet}$  is the vessel’s surface area in contact with the water,  $U_\infty$  is the cruise velocity and  $C_D$  is the skin friction drag coefficient in turbulent flow and high Reynolds number, given as an empirical approximation [28]:

$$C_D \approx \frac{0.03}{Re^{1/7}} \tag{15}$$

Reynolds number  $Re$  is related to the length of the submerged system and its influence on  $C_D$  and hence on  $D$  is weakly dependent on the cruise speed. Another important factor is that in order to overcome the drag in higher cruise velocities, the air-to-water mass ratio

$\mu$  has to increase. Because of the limitation on  $\alpha$  for bubbly flows,  $\mu$  should be limited as well. One may conclude that this propulsion system can easily overcome the vehicle drag at low to intermediate cruise speed range but may provide marginal excess thrust at the high-speed cruise range. As discussed before, the actual cycle performance may be lower than the ideal performance, depending on the specific operating conditions.

### 3. Experimental Vessel and Test Procedure

#### 3.1. General Description

The open-sea trials used a 405 Meteor boat, 4 m long and 1.95 m wide, manufactured by Alerplast, Kiryat Bialik, Israel, as a test platform. To the best of our knowledge, it has been the first time that a parametric examination of a two-phase marine ramjet, using a full-scale vessel in open-sea cruise conditions, has taken place. The boat was equipped with two submerged ramjet propulsion units attached to its bottom, an onboard turbo-compressor for air supply, control and data acquisition systems, pressure, airflow rate, and velocity measuring gauges, and auxiliary systems such as pneumatic starting unit. During sea trials, the boat was operated by two onboard persons: one for navigation and control and one for operating the turbo-compressor. Originally the boat was propelled by a 40 hp outboard engine enabling a maximum speed of 15 m/s (30 knots). When installing the submerged ramjet units, the outboard engine could not accelerate the boat to more than 10 m/s (20 knots) because of the increased resistance. According to Equation (7), the maximum ideal power that could be provided by the expanding air bubbles at the top airflow rate of 0.5 kg/s, is about 20 hp. Hence, it was evident that the ramjet power would not overcome the test vessel resistance in these conditions. In fact, it was a desirable situation, because the sea trials were planned for towing experiments, where a towing boat would tow our vessel at different speeds, and the thrust generated by the ramjet propulsion units would be measured in real-time according to the change in resistance. A general schematic illustration of the experimental vessel and test arrangement is presented in Figure 4.

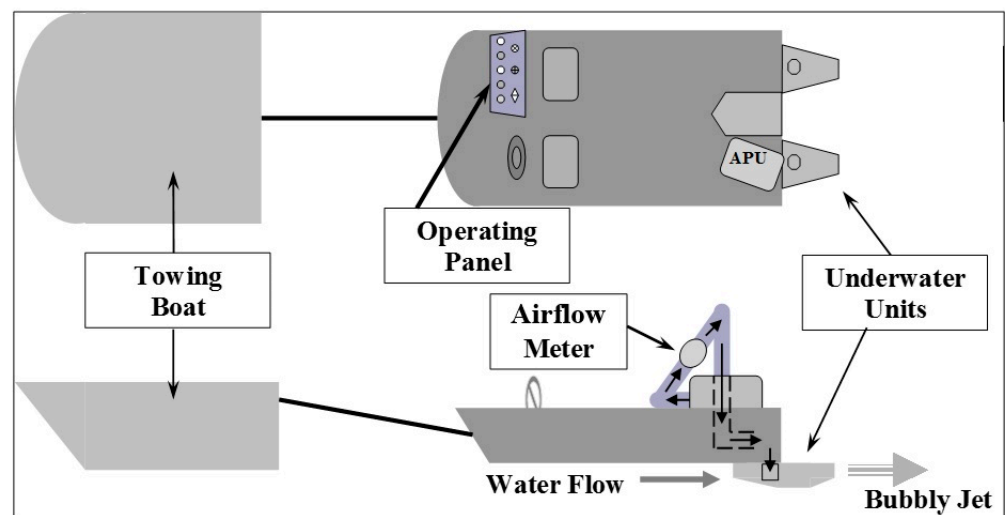


**Figure 4.** Schematic illustration of the general arrangement of the open-sea test vessel (top and side views).

The towing boat was Meteor 700, also manufactured by Alerplast, Kiryat Bialik, Israel, having a 400 hp engine and capable of 20 m/s (40 knots) cruise velocity; it could tow the test vessel at a velocity of up to 12.5 m/s (25 knots) along the test route. It also provided a comfortable work platform for the personnel involved in the operation besides the test vessel's crew. The towing boat crew operated the tension gauge attached to the towing cable, recorded the cruise speed using GPS, and kept eye contact with the test vessel to

ensure smooth operation and warn of problems. Figure 5 shows the test vessel and Figure 6 presents the towing boat.



Figure 5. Picture of the test vessel.



Figure 6. Picture of the towing boat.

### 3.2. The Underwater Ramjet Propulsion Units

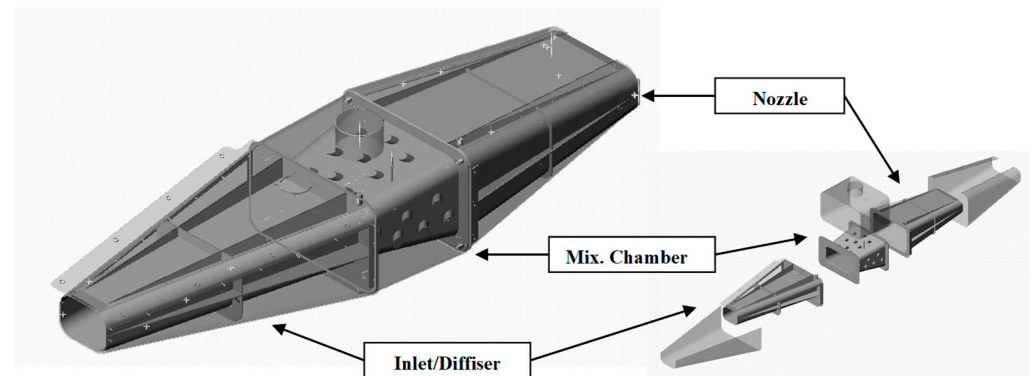
Two identical marine ramjet propulsion units were used. They were attached to the bottom of the test vessel at its rear end and were fully submerged during the operation. The units were designed to ingest water flow rate adjusted to establish a maximum volume fraction of the bubbles of about 70% at the exit cross-section for the maximum airflow rate of 0.5 kg/s (for the two units together) when cruising at 15 m/s (30 knots). It was revealed during the experiments that the actual cruise velocity during the open-sea testing was lower, of the order of 10 m/s (20 knots). The flow development (pressure and velocity) along the propulsion units was calculated according to the analysis presented by Mor and Gany [8]. The incoming water velocity was taken as the cruise speed, and the water flow rate was calculated accordingly (accounting for the inlet cross-section). The propulsion units had a rectangular cross-section to be adjusted to the flat vessel bottom. The inlet cross-section (index in) was designed to accommodate the desired incoming water flow rate at the entrance. The cross-section varied along the axial direction, enlarging the diffuser flow passage, slowing down the flow, and increasing the internal pressure at the mixing chamber (index mix). After the mixing section, the cross-section decreased gradually enabling expansion of the two-phase flow in the nozzle section, reaching the ambient pressure at the exit cross-section (index e). See again the different sections in Figure 1. The geometry of each of the two identical ramjet propulsion units is presented in Table 2.  $L_{dif}$  refers to the diffuser length from the inlet plane to the beginning of the mixing chamber.

**Table 2.** Geometric data of the underwater marine ramjet units <sup>1</sup>.

$A_{in}$	$A_{mix}$	$A_e$	$L_{dif}$	$L_{mix}$	$L_{nozzle}$
77.3	351.1	146.6	30	15	40

<sup>1</sup> Cross-section (A) in cm<sup>2</sup> and length (L) in cm.

One can see from Table 2 that the actual ratio of mixing chamber to inlet cross-sections is relatively large,  $A_{mix}/A_{in} = 4.54$ . It implies that the static pressure in the mixing chamber is very close to the stagnation pressure (almost 98% of  $P_t$  in the ideal case of no friction and mixing losses). A drawing of one propulsion unit is shown in Figure 7. The unit was made of stainless steel. The mixing chamber section had a double wall, where air from the turbo-compressor was supplied through a 4" pipe into the volume created between the two walls, entering the mixing chamber via multiple 20 mm diameter ports. One may assume that the entering air jets would break up, generating a broad size distribution of bubbles in the interior flow. The mixing chamber had a gradually increasing cross-section to maintain a constant flow velocity during the distribution of the incoming air along the mixing section. The two-phase bubbly flow would then expand along the converging nozzle section forming a high-speed two-phase exhaust jet.

**Figure 7.** The underwater ramjet propulsion unit structure.

### 3.3. The Compressed Air Supply Assembly

The core of the compressed air production and supply complex was a NAVAIR WR27-1 turbo-compressor installed on the test boat. This gas turbine system was originally used as an airborne system, Auxiliary Power Unit—APU, to start turbo-jet engines of the US Navy aircraft. It was purchased from a used-part yard after refurbishment and was installed at the stern area of the vessel. A shield was constructed around the unit to protect it from seawater fog and splash and to protect the operating crew from the high noise. The turbo-compressor weighed 60 kg. It operated at 64,000 rpm at full power and could supply up to 0.6 kg/s of air at an absolute pressure of 3 bar. The air was split by a division valve and channeled through stainless-steel piping at equal flow rates into the two underwater propulsion units.

The gas turbine was started using a hydraulic starting system—a two-stroke engine that compressed oil in a hydraulic accumulator to a pressure of 3000 psi (approximately 200 bar). When a start signal was given, the pressure in the accumulator was released to create a rotational motion in the turbine. The starting system could increase the turbine rotation rate to a value of about 12,000 rpm. If, at the same time of the start signal, an ignition signal is also given and the jet fuel begins to burn, the engine rotation rate increases to a value of about 64,000 rpm, which is the working range of the turbine.

The use of a gas turbine system operating at high rotation speeds required the development of a sophisticated and safe control panel that allowed control of all parameters. The control panel was located at the bow near the steering wheel, allowing the turning of the gas turbine on and off, and providing the operator control over the airflow delivered to

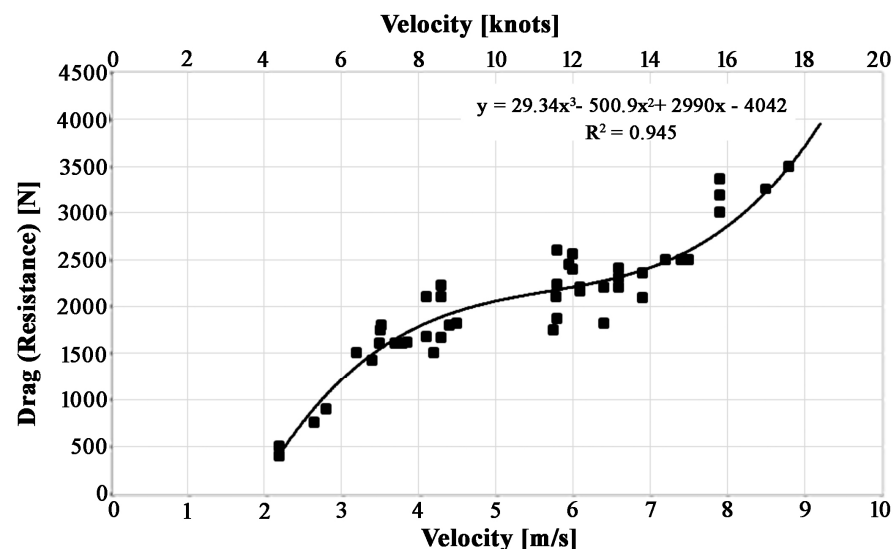
the underwater units. The system provided indications of safety parameters such as the turbine rpm, the turbine exhaust pipe temperature (TTP), and the engine pressure. Safety automatic shutdown of the engine would occur in two cases: (1) at a temperature rise in the gas-turbine exhaust pipe exceeding 1400 °F, which indicates a load in the system; (2) when the turbine rpm exceeds 66,000 rpm. In addition to the safety parameters, the control panel also provided control over the discharge valves, which determined the level of airflow entering the underwater units.

### 3.4. Sea Trial Procedure and Measurements

As mentioned before, the sea trials consisted of towing experiments measuring the resistance sensed by a strain gauge attached to the towing cable connecting the two boats. An escort boat with a skilled crew accompanied the test vessel during the cruise experiments to provide aid if problems arose. Cruise velocity was measured by a GPS device providing an immediate indication of the speed of the vessel. The first series of sea trials provided reference data on the resistance versus cruise velocity when the ramjet propulsion units were shut off. Further series of experiments took place when the ramjet propulsion units were operating at two levels of airflow supply, 0.275 kg/s and 0.500 kg/s (with flow rate fluctuations of up to 0.025 kg/s), measured by a Model 454FT-08-MT flow meter of Kurz Instruments (accuracy  $\pm 3\%$  of the reading). When the ramjet units were operating, the measured resistance was of course lower than in the case of no ramjet operation. The difference between the measured resistance indicated the thrust generated by the two-phase marine ramjet units. Additional measurements during testing were air temperature (accuracy  $\pm 1$  °C) and pressure using two analog 0–60 psig (0–4 bar gauge) transducers (accuracy  $\pm 0.1$  bar) at the entrance to the underwater units.

## 4. Results and Discussion

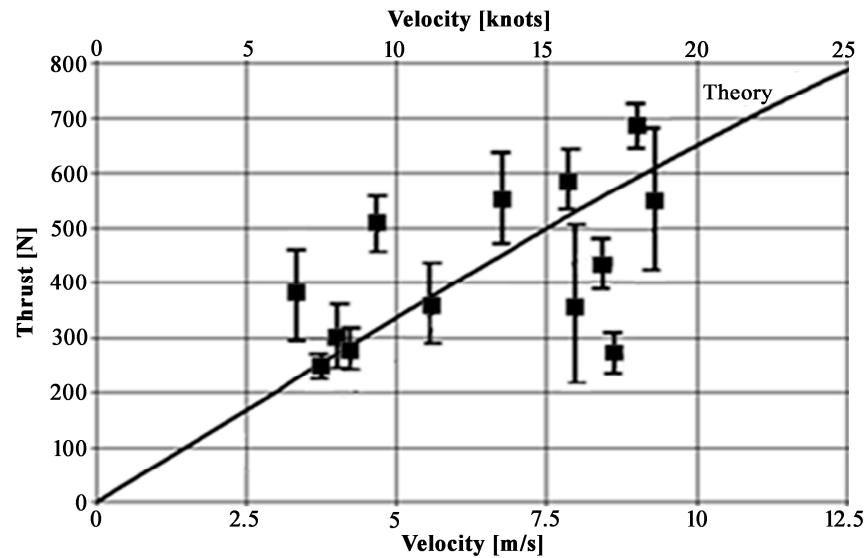
The baseline resistance curve was determined over a range of cruise velocities, towing the test vessel with the ramjet propulsion units off. The resistance line (a reference curve) is presented in Figure 8.



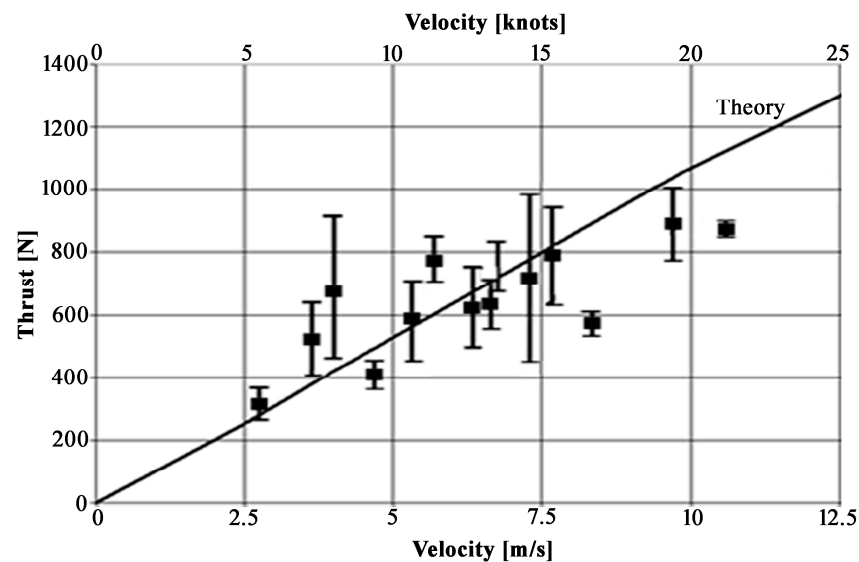
**Figure 8.** The reference resistance curve of the test vessel vs. cruise velocity for non-operating ramjet propulsion units. The figure displays the test points as well as an empirical correlation.

Figure 9 presents the test results of thrust versus cruise velocity obtained from the open-sea trials at an air supply of 0.275 kg/s. A similar plot is presented in Figure 10 for an airflow rate of 0.500 kg/s. The results reveal good correspondence with the theoretical thrust curve calculated according to Equation (10) with no expansion losses. Some scattering of the results can be observed. It may result from several reasons: First, the sea conditions,

waves, wind, etc., may vary from test to test. Second, as mentioned above, the reference resistance curve itself shows possible errors as high as 300 N, implying uncertainty of the same order in the thrust determination. Another factor is the fluctuations of airflow rate which can be as high as 5–10%. Nevertheless, one should note the relatively good correspondence of the average test results with the theoretical prediction.



**Figure 9.** Test data and theoretical prediction of the underwater ramjet thrust vs. cruise velocity for airflow rate of 0.275 kg/s. The theoretical prediction was calculated according to the ideal isothermal expansion work of the air.



**Figure 10.** Test data and theoretical prediction of the underwater ramjet thrust vs. cruise velocity for airflow rate of 0.500 kg/s. The theoretical prediction was calculated according to the ideal isothermal expansion work of the air.

According to the air and water flow rates, it seems that the air-to-water mass ratio  $\mu$  in the sea trials was roughly within the range of bubbly flows when the air supply was 0.275 kg/s, and may have exceeded that range for the 0.500 kg/s. The main reason was that the propulsion units were designed for work conditions of 15 m/s (30 knots) and in practice only about 10 m/s could be achieved because of the large additional resistance imposed by the submerged ramjet units. Interestingly, the results revealed that the bubbly flow model could give reasonable prediction also for the higher  $\mu$ , though the test results at the

high cruise velocity range demonstrated some points that were somewhat lower than the predicted theoretical curve. It is noted that optimized operation of the two-phase marine ramjet over broad ranges of cruise velocity and thrust could generally be accomplished by using a nozzle with a controlled variable exit cross-section as well as a variable air supply. Though it is a feasible arrangement, a variable nozzle is rarely considered in actual waterjet propulsion. The predicted thrust for an extended cruise speed range of up to 25 m/s (50 knots) for both airflow rates of 0.275 kg/s and 0.500 kg/s is presented in Figure 11. One can see that the thrust is expected to increase monotonically with the cruise speed. However, the gradient of thrust enhancement decreases at the higher speed range.

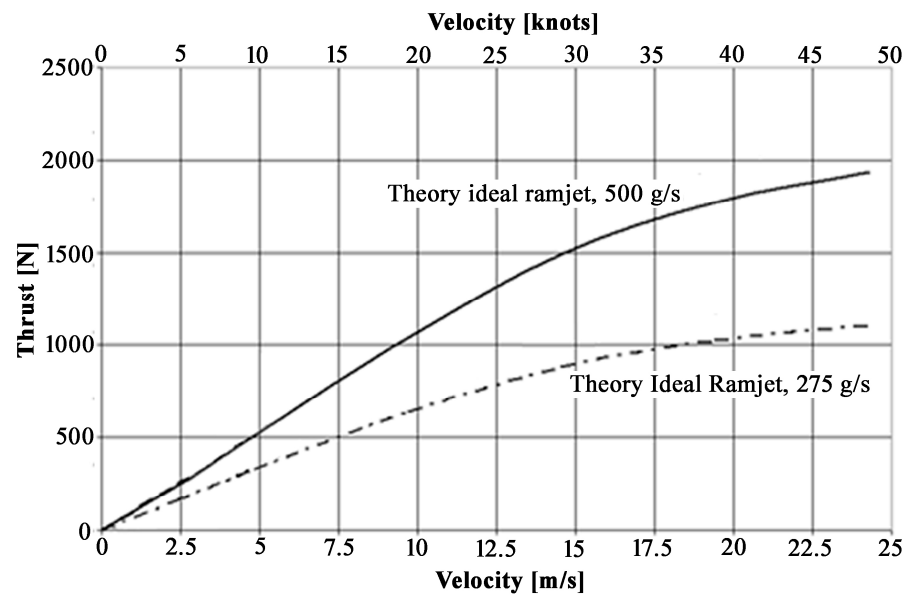


**Figure 11.** The predicted thrust for extended cruise speed range at different airflow rates (indicated near the curves).

## 5. Conclusions

This research presents a comprehensive investigation of the marine two-phase ramjet propulsion in real open-sea trials of a full-scale vehicle. To the best of our knowledge, it is the first time for such a test campaign. The experiments were backed by theoretical analysis and prediction, showing fairly good correspondence with some test scattering resulting from the measurement uncertainty and instrumentation errors, test-to-test variation due to the sea conditions, and fluctuation of air supply. The main conclusions are:

- The theoretical thermodynamic cycle assuming the transfer of the isothermal expansion work of the air bubbles within the two-phase flow to the water, can serve as the basis for the marine two-phase ramjet propulsion.
- The two-phase ramjet propulsion can yield a higher thrust margin versus the vessel resistance at the low to intermediate cruise speed range than at very high speeds.
- The thrust demonstrated in actual sea trials corresponds fairly well with the theoretical prediction of the ideal operation.
- According to the actual sea trials, performance prediction assuming a bubbly flow regime may be roughly applied for higher air-to-water flow rate ratios as well, though with lower accuracy.
- Summarizing the research, the two-phase marine ramjet may be a viable and predictable marine propulsion concept.

**Author Contributions:** Conceptualization, A.G.; Methodology, S.V. and A.G.; Validation, S.V. and A.G.; Formal analysis, A.G.; Investigation, S.V. and A.G.; Data curation, S.V.; Writing—original draft, S.V. and A.G.; Writing—review & editing, A.G.; Supervision, A.G. All authors have read and agreed to the published version of the manuscript.

**Funding:** This research received no direct external funding.

**Institutional Review Board Statement:** Not applicable.

**Informed Consent Statement:** Not applicable.

**Data Availability Statement:** All relevant data are detailed in the article.

**Acknowledgments:** The authors acknowledge the substantial technical aid of Avraham Valensi and Oren Koren and the long-time support of Ron Goldschlager, Managing Director, the Hermal Mortim Group.

**Conflicts of Interest:** The authors declare no conflict of interest.

## References

1. Tangren, R.F.; Dodge, C.H.; Seifert, H.S. Compressibility effects in two-phase flow. *J. Appl. Phys.* **1949**, *20*, 637–645. [[CrossRef](#)]
2. Muir, J.H.; Eichhorn, R. Compressible Flow of an Air-Water Mixture Through a Vertical, Two-Dimensional, Converging-Diverging Nozzle. In Proceedings of the Heat Transfer and Fluid Mechanics Institute, Pasadena, CA, USA, 12–14 June 1963; pp. 183–204.
3. Soo, S.L. *Multiphase Fluid Dynamics*; Science Press: Beijing, China, 1990.
4. Wallis, G.B. *One-Dimensional Two-Phase Flow*; McGraw-Hill: New York, NY, USA, 1969.
5. Van Wijngaarden, L. One-dimensional flow of liquids containing small gas bubbles. *Annu. Rev. Fluid Mech.* **1972**, *4*, 369–394. [[CrossRef](#)]
6. Brennen, C.E. *Cavitation and Bubble Dynamics*, 2nd ed.; Cambridge University Press: Cambridge, UK, 2005.
7. Albagli, D.; Gany, A. High speed bubbly nozzle flow with heat, mass, and momentum interactions. *Int. J. Heat Mass Trans.* **2003**, *46*, 1993–2003. [[CrossRef](#)]
8. Mor, M.; Gany, A. Analysis of two-phase homogeneous bubbly flows including friction and mass addition. *J. Fluid Eng.* **2004**, *126*, 102–109. [[CrossRef](#)]
9. Mottard, E.J.; Shoemaker, C.J. *Preliminary Investigation of an Underwater Ramjet Powered by Compressed Air*; NASA TN D-991; Langley Research Center: Hampton, VA, USA, 1961.
10. Witte, J.H. Predicted Performance of Large Water Ramjet. In Proceedings of the AIAA 22d Advanced Marine Vehicles and Propulsion Meeting, Seattle, WA, USA, 21–23 May 1969.
11. Albagli, D.; Gany, A. Analysis of a High-Speed Bubbly Waterjet. In Proceedings of the 28th AIAA/SAE/ASME/ASEE Joint Propulsion Conference, Nashville, TN, USA, 6–8 July 1992.
12. Varshay, H.; Gany, A. Underwater Two-Phase Ramjet Engine. U.S. Patent 5,598,700A, 4 February 1997.
13. Varshay, H.; Gany, A. Underwater Two-Phase Ramjet Engine. U.S. Patent 5,692,371A, 2 December 1997.
14. Gany, A. Analysis of a New Thermodynamic Power Cycle for a Two-Phase Waterjet. In Proceedings of the International Conference Waterjet Propulsion 4, The Royal Institute of Naval Architects (RINA), London, UK, 26–27 May 2004.
15. Pierson, J.D. An Application of Hydrodynamic Propulsion to Hydrofoil Craft. In Proceedings of the 1st AIAA Annual Meeting, Washington, DC, USA, 29 June–2 July 1964.
16. Mor, M.; Gany, A. Performance mapping of bubbly water ramjet. *Int. J. Marit. Eng.* **2007**, *149*, 45–50. [[CrossRef](#)]
17. Chahine, G.L.; Hsiao, C.-T.; Choi, J.-K.; Wu, X. Bubble Augmented Waterjet Propulsion: Two-Phase Model Development and Experimental Validation. In Proceedings of the 27th Symposium on Naval Hydrodynamics, Seoul, Republic of Korea, 5–10 October 2008; pp. 1127–1143.
18. Singh, S.; Fourmeau, T.; Choi, J.K.; Chahine, G.L. Thrust enhancement through bubble injection into an expanding–contracting nozzle with a throat. *J. Fluids Eng.* **2014**, *136*, 071101-1–071101-10. [[CrossRef](#)]
19. Wu, X.; Choi, J.-K.; Leaman Nye, A.; Chahine, G.L. Effect of Nozzle Type on the Performance of Bubble Augmented Waterjet Propulsion. In Proceedings of the 4th International Symposium on Marine Propulsors (SMP'15), Austin, TX, USA, 31 May–4 June 2015; pp. 122–134.
20. Gowing, S.; Mori, T.; Neely, S. Research on two-phase waterjet nozzles. *J. Fluids Eng.* **2010**, *132*, 121302. [[CrossRef](#)]
21. Fu, Y.-J.; Wei, Y.-J.; Zhang, J.-Z. Parametric study on the thrust of bubbly water ramjet with a converging-diverging nozzle. *J. Hydrodyn.* **2009**, *21*, 591–599. [[CrossRef](#)]
22. Liu, D.; Li, S.; Xie, G. Effect of primary water injection angle on thermal propulsion performance of a water ramjet engine, *Aerosp. Sci. Technol.* **2020**, *97*, 105630. [[CrossRef](#)]
23. Zhang, J.; Xia, Z.; Huang, L.; Ma, L. Experimental and numerical parametric studies on two-phase underwater ramjet. *J. Propul. Power* **2018**, *34*, 161–169. [[CrossRef](#)]
24. Eisen, N.E.; Gany, A. Theoretical performance evaluation of a marine solid propellant water-breathing ramjet propulsor. *J. Mar. Sci. Eng.* **2020**, *8*, 8. [[CrossRef](#)]
25. Eisen, N.E.; Gany, A. Examining metal additives in a marine hybrid propellant water-breathing ramjet. *J. Mar. Sci. Eng.* **2022**, *10*, 134. [[CrossRef](#)]
26. Eisen, N.E.; Gany, A. Investigation of a marine water-breathing hybrid ram-rocket motor. *J. Propul. Power* **2022**, *38*, 370–377. [[CrossRef](#)]

27. Frolov, S.M.; Avdeev, K.A.; Aksenov, V.S.; Frolov, F.S.; Sadykov, I.A.; Shamshin, I.O. Pulsed detonation hydramjet: Design optimization. *J. Mar. Sci. Eng.* **2022**, *10*, 1171. [[CrossRef](#)]
28. Hoerner, S.F. *Fluid Dynamic Drag—Practical Information on Aerodynamic Drag and Hydrodynamic Resistance*, 2nd ed.; Hoerner Fluid Dynamics: Brick Town, NJ, USA, 1965; Chapter 2; pp. 2–5.

**Disclaimer/Publisher’s Note:** The statements, opinions and data contained in all publications are solely those of the individual author(s) and contributor(s) and not of MDPI and/or the editor(s). MDPI and/or the editor(s) disclaim responsibility for any injury to people or property resulting from any ideas, methods, instructions or products referred to in the content.